



HAL
open science

Using remotely sensed solar radiation data for reference evapotranspiration estimation at a daily time step

Benjamin Bois, Philippe Pieri, Cornelis van Leeuwen, Lucien Wald, Frédéric Huard, Jean-Pierre Gaudillère, Etienne Saur

► To cite this version:

Benjamin Bois, Philippe Pieri, Cornelis van Leeuwen, Lucien Wald, Frédéric Huard, et al.. Using remotely sensed solar radiation data for reference evapotranspiration estimation at a daily time step. *Agricultural and Forest Meteorology*, 2007, 148 (4), pp.619-630. 10.1016/j.agrformet.2007.11.005 . hal-00335548

HAL Id: hal-00335548

<https://hal.science/hal-00335548>

Submitted on 29 Nov 2008

HAL is a multi-disciplinary open access archive for the deposit and dissemination of scientific research documents, whether they are published or not. The documents may come from teaching and research institutions in France or abroad, or from public or private research centers.

L'archive ouverte pluridisciplinaire **HAL**, est destinée au dépôt et à la diffusion de documents scientifiques de niveau recherche, publiés ou non, émanant des établissements d'enseignement et de recherche français ou étrangers, des laboratoires publics ou privés.

Using remotely sensed solar radiation data for reference evapotranspiration estimation at a daily time step

B. Bois^a, P. Pieri^a, C. Van Leeuwen^{b,*}, L. Wald^c, F. Huard^d, J.-P. Gaudillere^a, E. Saur^b

^aUMR Ecophysiologie et Génomique Fonctionnelle de la Vigne, ISVV, Université Bordeaux 2 - INRA, BP 81,
33883 Villenave d'Ornon Cedex, France

^bEcole Nationale d'Ingénieurs des Travaux Agricoles de Bordeaux, 1 cours du Général de Gaulle, 33175
Gradignan Cedex, France

^cCEP, Ecole de Mines de Paris, BP 207, F-06904 Sophia Antipolis Cedex, France

^dUE AgroClim, INRA, Domaine de Saint-Paul, Site Agroparc, 84914 Avignon Cedex 9, France

*Corresponding author, Tel.: +33 5 57 35 07 55; Fax: +33 5 57 35 07 59. Email: k-van-leeuwen@enitab.fr

Abstract

Solar radiation is an important climatic variable for assessing reference evapotranspiration (E_0), but it is seldom available in weather station records. Meteosat satellite images processed with the Heliosat-2 method provide the HelioClim-1 database, which displays spatialized solar radiation data at a daily time step for Europe and Africa. The aim of the present work was to investigate the interest of satellite-sensed solar radiation for E_0 calculation, where air temperature is the sole local weather data available. There were two study areas in Southern France. One (Southwest, SW) is characterized by oceanic climate and the other (Southeast, SE) by Mediterranean climate. A data set of daily values for 19 weather stations spanning five years (2000–2004) was used. First, a sensitivity analysis of the Penman-Monteith formula to climate input variables was performed, using the Sobol' method. It shows that E_0 is mainly governed by solar radiation during summer, and by wind speed during winter. Uncertainties of HelioClim-1 solar radiation data and their repercussions on E_0 formulae were evaluated, using the FAO-56 Penman-Monteith formulae (PM) and radiation-based methods (Turc, TU ; Priestley-Taylor, PT and Hargreaves-Radiation, HR). It was shown that HelioClim-1 data slightly underestimate solar radiation and provide relative RMSE (root mean squared error) of 20% of the mean annual value for SW and 14% for SE. The propagation of HelioClim-1 data uncertainties is small in PM but considerable in radiation methods. Four estimation methods were then compared to PM data: the 1985 Hargreaves formula (HT) based on air temperature only; TU , PT and HR , based on air temperature and satellite sensed solar radiation. Radiation methods were more precise and more accurate than HT , with RMSE ranging from 0.52 mm to 0.86 mm against 0.67 mm to 0.96 mm. These results suggest that using satellite-sensed solar radiation may improve E_0 estimates for areas where air temperature is the only available record at ground level.

Keywords: evapotranspiration, solar radiation, Penman-Monteith equation, sensitivity analysis, remote sensing.

1 Introduction

Reference evapotranspiration (E_0) is an agrometeorological variable widely used in hydrology and agriculture. Together with precipitation, it is a major input in soil water balance models. Several of these models require daily or hourly evapotranspiration data to provide acceptable estimate of plants water requirements (Brisson et al., 1992 ; Guyot, 1997 ; Lebon et al., 2003). Penman-Monteith combination method is one of the most accurate methods to evaluate E_0 at different time steps. A standardization of this method has been proposed by the Food and Agriculture Organization (Allen *et al.*, 1998). It is known as FAO-

52 56 Penman-Monteith application, and it can be considered as a worldwide standard. However,
53 it requires numerous weather variables (air temperature, relative humidity, wind speed and
54 solar radiation), which are seldom available in basic meteorological records. Consequently,
55 reference evapotranspiration is often estimated by means of empirical equations based on air
56 temperature, relative humidity, extraterrestrial radiation and/or precipitation (Droogers and
57 Allen, 2002 ; Hargreaves et al., 1985 ; Popova et al., 2005 ; Turc, 1961). Several authors
58 proposed modifications of existing empirical methods (Droogers and Allen, 2002 ; Gavilan et
59 al., 2006 ; Pereira, 2004 ; Pereira and Pruitt, 2004 ; Popova et al., 2005 ; Xu and Singh, 2002).
60 The accuracy of these methods remains acceptable when applied at large time and space
61 scales (e.g., a decade and distances larger than 1000 km). However, empirical formulae are
62 limited by their inherent characteristics. The lack of one, or more, climate variable physically
63 related to evaporation and transpiration processes inescapably reduces the accuracy of
64 evapotranspiration estimation. Even if recalibration of empirical factors may improve locally
65 the precision of these methods, considerable estimation errors will remain as time variations
66 of missing climate variables are not considered. An example of this statement is the varying
67 behavior of empirical formulae according to the type of climate considered (Jensen et al.,
68 1990). Thus, there is little hope that a universal, accurate and robust empirical formula based
69 on a limited set of weather variables will ever be proposed.

70 Choudhury (1997) proposed a method to assess E_0 by means of satellite data, such as remotely
71 sensed solar radiation, air temperature (derived from infrared images and weather station
72 measurements) and vapor pressure deficit. This method provides good evapotranspiration
73 estimates for low-resolution applications such as worldwide scale and monthly time step. The
74 accuracy is limited by the high uncertainties provided by satellite sensed vapor pressure
75 estimations.

76 Several methods have been recently proposed to estimate solar radiation (Struzik, 2001).
77 Amongst them, the Heliosat-2 method (Rigollier *et al.*, 2004) has been proved to be
78 reasonably reliable for estimating daily irradiation over Europe and Africa. This method has
79 been used to elaborate a database, HelioClim-1, available at <http://www.soda-is.org> (Lefèvre
80 *et al.*, 2007).

81 Solar radiation strongly controls evaporation from the land surface. As small uncertainties in
82 solar radiation may have considerable effect on the E_0 calculation (Llasat and Snyder, 1998)
83 and as the variations in space of the radiation cannot be captured by pyranometers, which are
84 in any case expensive and fragile devices, it can be assumed that remotely sensed solar
85 irradiation should be useful for E_0 estimation.

86 In this paper, the relevance of remotely sensed solar radiation for computing E_0 at a daily time
87 step is tested and discussed. First, a sensitivity analysis of the Penman-Monteith method to
88 input variables for daily reference evapotranspiration calculation is performed. Then satellite-
89 sensed solar radiation data is compared to ground data and error propagations in several E_0
90 methods are evaluated. Finally, the accuracy of several E_0 methods based on solar radiation
91 data are compared to the E_0 Hargreaves temperature method, to evaluate the benefits provided
92 by the use of satellite-sensed solar radiation, for areas where air temperature is the only
93 ground-measured available data.

94 95 **2 Methods**

96 97 *2.1 Study areas*

98 The study was performed in two regions of France (figure 1). One is located in the Southwest
99 of France (hereafter referred to as SW). It is mostly flat and is characterized by a temperate
100 climate under the influence of the Atlantic Ocean. Rainfalls range from 800 mm to 1800 mm
101 per year; the average value for the area is 1000 mm per year. Summer is dry (mean of 60 mm
per month), and autumn and winter are wet (approximately 100 mm per month). From 1971

102 to 2000, monthly means of temperatures varied from 5 °C in the winter to 20 °C in the
103 summer. The second area is the Southeast of France (hereafter referred to as SE). It exhibits
104 marked orography due to the Southern Alps. The climate is Mediterranean, with hot and dry
105 summers (20 mm to 40 mm of rainfall per month and an average maximum temperature over
106 30 °C) and mild and wetter winters (40 mm to 100 mm per month with mean temperature
107 between 0 °C and 5 °C).

108 2.2 Data

109 2.2.1 Ground station data

110 Data was collected from 19 INRA-Agroclim weather stations. Eight are situated in Southwest
111 area and 11 are located in Southeast area (table 1 and figure 1). All stations are Cimel[®]
112 automatic weather stations, equipped with humidity and thermal sensors under a cylinder type
113 disc shelter (80 mm x 150 mm), cup anemometer and class 2 pyranometer. Minimum and
114 maximum temperature, minimum and maximum relative humidity, solar irradiation and wind
115 speed at 2 meters high at a daily time step were used. Average daily temperature is the mean
116 of minimum and maximum daily temperatures values. The study was performed on a five
117 year (2000-2004) data set.

118 2.2.2 Satellite sensed solar radiation

119 Remotely sensed solar irradiation was collected from the HelioClim-1 database available at
120 <http://www.soda-is.org>. This database has been obtained by the application of the Heliosat-2
121 method to Meteosat satellite images. The Heliosat-2 method is based on the principle of the
122 construction of a *cloud index* for each given pixel of satellite images (Cano *et al.*, 1986 ;
123 Rigollier *et al.*, 2004). This index is obtained by calculating ground and cloud albedos from
124 time-series of images acquired in a broadband channel spanning visible and near-infrared
125 bands. A clear-sky index is then derived from the cloud index. Irradiation is obtained by
126 multiplying this clear-sky index by the irradiation that should be observed under clear-sky
127 conditions; the latter is estimated by means of the model of Rigollier *et al.* (2000). The
128 precision of the method depends mostly on the cloud cover: relative uncertainties are lower
129 during clear sky days (Rigollier *et al.*, 2004 ; Lefèvre *et al.*, 2007).

130 The HelioClim-1 database provides daily irradiation data for Europe and Africa. It has been
131 constructed from a data set of reduced spatial resolution, called ISCCP-B2 data, that was
132 created for the International Satellite Cloud Climatology Project (ISCCP) to better handle and
133 exploit the wealth of information provided by the Meteosat series of satellites. The B2 data set
134 is produced from Meteosat images by firstly performing a time sampling that reduces the
135 frequency of observation to the standard meteorological synoptic 3-h intervals, starting at
136 0000 UTC. Secondly, the higher-resolution data in the visible channel are averaged to match
137 the lower resolution of infrared channel data (i.e. an image of 2500 x 2500 pixels with a
138 resolution of 5 km). Finally, a spatial sampling is performed by taking 1 pixel over 6 in each
139 direction (i.e. 1 pixel each 30 km), starting with the south-easternmost pixel. For each
140 remaining pixel, the irradiation was calculated every 3 h and integrated to provide daily
141 irradiation. The HelioClim-1 database contains daily irradiation for these pixels (Lefevre et
142 al., 2007). The irradiation data for any location are obtained by interpolating the daily values
143 available at the nine closest pixels using inverse distance squared method (Lefèvre *et al.*,
144 2002). Daily irradiation data were collected for the location of the 19 weather stations for the
145 period 2000-2004.

146 2.3 Reference evapotranspiration methods

147 2.3.1 The FAO Penman-Monteith method

148

151 The Penman-Monteith method combines energy balance and mass transfer concepts (Penman,
 152 1948) with stomatal and surface resistance (Monteith, 1981).
 153 Recently, the FAO proposed a standard parameterization of the Penman-Monteith method for
 154 estimating the evaporation from a well-irrigated, homogenous, 0.12 m grass cover considered
 155 as a “reference crop” (Allen *et al.*, 1998). This method, hereafter referred as *PM*, is now used
 156 worldwide and the international agronomy community considers it as a standard. The FAO
 157 Penman-Monteith reference evapotranspiration (mm) is calculated as follows:

$$158 \quad E_{PM} = \frac{0.408\Delta(R_n) + \gamma \frac{900}{(T + 273)} u_2 (e_s - e_a)}{\Delta + \gamma(1 + 0.34u_2)} \quad (1)$$

159 where Δ is the slope of the saturation vapor pressure curve at air temperature [kPa °C⁻¹], γ is
 160 the psychrometric constant [kPa °C⁻¹], T is the average air temperature [°C], u_2 is the wind
 161 speed measured at 2 m above ground surface [m s⁻¹], e_s and e_a are the saturation and the actual
 162 vapor pressure [kPa], respectively, and R_n is the net radiation [MJ m⁻²], calculated as follows :

$$163 \quad R_n = R_{ns} - R_{nl} \quad (2)$$

164 where R_{ns} is the net shortwave radiation [MJ m⁻²] given by :

$$165 \quad R_{ns} = (1 - a)R_s \quad (3)$$

166 and R_{nl} is the net longwave radiation [MJ m⁻²] given by :

$$167 \quad R_{nl} = \sigma \left[\frac{T_{\max,K}^4 + T_{\min,K}^4}{2} \right] \left(0.34 - 0.14\sqrt{e_a} \right) \left(1.35 \frac{R_s}{R_{so}} - 0.35 \right) \quad (4)$$

168 where R_s is the global solar radiation [MJ m⁻²], a is the albedo of the hypothetical grass
 169 reference crop, set to 0.23, $T_{\max,K}$ and $T_{\min,K}$ are the maximum and minimum air temperature
 170 [K], respectively, and R_{so} is the clear-sky solar radiation [MJ m⁻²], given by :

$$171 \quad R_{so} = (0.75 + 2z10^{-5})R_a \quad (5)$$

172 where z is the station elevation above sea level [m] and R_a is the extraterrestrial radiation
 173 [MJ m⁻²]. Undefined components used in equations (2), (3), (4) and (5) have the same
 174 signification and units as in equation (1).

175 The actual vapor pressure [kPa], used in equations (1) and (4) is calculated as follows:

$$176 \quad e_a = \frac{e^{\circ}(T_{\min}) \frac{RH_{\max}}{100} + e^{\circ}(T_{\max}) \frac{RH_{\min}}{100}}{2} \quad (6)$$

177 where $e^{\circ}(T_{\min})$ and $e^{\circ}(T_{\max})$ are the saturation vapor pressure at minimum and maximum air
 178 temperature [kPa], respectively, RH_{\min} is the minimum relative humidity and RH_{\max} is the
 179 maximum relative humidity.

180 The slope of saturation vapor pressure curve at air temperature is given by :

$$181 \quad \Delta = \frac{4098[e^{\circ}(T)]}{(T + 237.2)^2} \quad (7)$$

182 where $e^{\circ}(T)$ is the saturation vapor pressure at average air temperature and T as the same
 183 signification and units as in equation (1).

184 *PM* or other Penman-Monteith versions have been proved to be among the most precise and
 185 accurate models for daily reference evapotranspiration prediction under different climatic
 186 conditions when compared to lysimetric measurements (Allen *et al.*, 1989 ; Hargreaves and
 187 Allen, 2003 ; Garcia *et al.*, 2004 ; Pereira, 2004; Pereira and Pruitt, 2004).

188 In this paper, E_{PM} is considered as the reference value against which other empirical methods
 189 will be compared. This choice is motivated by the fact that most of the applications based
 190 upon reference evapotranspiration, such as irrigation schemes, hydrological studies or water
 191 balance modelling, use calculated E_0 rather than lysimetric measurements.

192

193 2.3.2 Empirical methods

194 In this study, radiation methods, *i.e.* empirical methods that calculate E_0 with air temperature
195 and solar radiation, are singled out, in order to test the relevance of using remotely sensed
196 solar radiation for E_0 estimates.

197 Three radiation methods and one temperature method were compared to *PM*.

198 Hargreaves radiation method (hereafter referred as to *HR*, Hargreaves and Samani, 1982) was
199 established in 1975 from a regression with lysimeter data collected at Davis (California, USA)
200 and the product of temperature and solar radiation, for a five day time step. The following
201 prediction equation was then proposed:

$$202 \quad E_{HR} = 0.0135 \frac{R_s}{\lambda} (T + 17.8) \quad (8)$$

203 where λ is the latent heat of vaporization = 2.45 MJ kg⁻¹ at 20 °C (as λ is very stable, this
204 value was used in the current study), and other components having the same signification and
205 units as in equations (1) and (3). Hargreaves radiation method has seldom been tested, despite
206 encouraging results (Hargreaves and Allen, 2003). As solar radiation has rarely been
207 available, Hargreaves proposed a modified version of this method, so that reference
208 evapotranspiration could be estimated with minimum and maximum air temperature only
209 (Hargreaves *et al.*, 1985). This method is known as the 1985 Hargreaves temperature method
210 (hereafter referred to as *HT*):

$$211 \quad E_{HT} = 0.0023 \frac{R_a}{\lambda} (T + 17.8) \sqrt{(T_{\max} - T_{\min})} \quad (9)$$

212 where T_{\min} and T_{\max} are the minimum and the maximum air temperature, respectively [°C].
213 and undefined components having the same signification and units as in equations (1), (5) and
214 (8). Local calibrations of the empirical coefficient (0.0023), based upon regional wind speed
215 and air temperature, were recently proposed (Gavilan *et al.*, 2006).

216

217 The Turc radiation method (hereafter referred to as *TU*; Turc, 1961), initially developed for
218 10-day periods, provides good results for a humid environment (Jensen *et al.*, 1990).

219 Reference evapotranspiration is calculated as follows:

$$220 \quad E_{TU} = 0.013 (23.88 R_s + 50) \left(\frac{T}{T + 15} \right) \quad (10)$$

221 where R_s and T have the same signification and units as in equations (1) and (3).

222 The Priestley-Taylor method (hereafter referred as *PT*, Priestley and Taylor, 1972), unlike
223 radiation methods presented above, is mostly based on physical principles. The *PT* method is
224 derived from energy balance concepts and the hypothesis that (at least for short vegetation)
225 fluxes over land are mostly governed by radiative rather than advected energy. Thus, E_0 is
226 given by:

$$227 \quad E_{PT} = \alpha \frac{\Delta}{\Delta + \gamma} R_n \quad (11)$$

228 where α is an empirical and unitless coefficient, set to 1.26, and R_n , Δ and γ have the same
229 signification and units as in equation (1). To avoid the use of minimum and maximum relative
230 humidity for E_{PT} calculation (E_{PT} is calculated with air temperature and solar radiation only),
231 the actual vapour pressure e_a , required for R_n calculation (equation (4)) is estimated from
232 minimum air temperature only:

$$233 \quad e_a = e^\circ(T_{\min}) = 0.611 \exp \left[\frac{17.27 T_{\min}}{T_{\min} + 237.3} \right] \quad (12)$$

234 where e_a and T_{\min} have the same significance and units as in equations (6) and (9).

235 Equation (12) follows the recommendations in Allen *et al.* (1998) to compute e_a when relative
 236 humidity is missing.
 237 *PT* method has been used and tested in many studies, and has shown to be reliable in humid
 238 climate conditions for evaporation (Xu and Singh, 2000) and reference evapotranspiration
 239 (Jensen *et al.*, 1990) estimations. Local adjustments of α are necessary in numerous cases (Xu
 240 and Singh, 2002; Bois *et al.*, 2005; Fisher *et al.*, 2005), and a calculation method for α based
 241 on surface and aerodynamic resistance parameters was proposed by Pereira (2004). A
 242 recalibration of α to increase the precision of *PT* estimates, is discussed in the results section,
 243 but the results presented in this paper focus on the *PT* method with α set to 1.26, as
 244 recalibration of empirical formulae is not the main objective of the present study.
 245

246 2.4 Sensitivity analysis

247 2.4.1 The Sobol' method

248 To estimate the relative participation of climate variables to *PM* model output, a sensitivity
 249 analysis was performed. There are several approaches available for sensitivity analysis studies
 250 (see Frey and Patil, 2002 or Saltelli *et al.*, 2006 for reviews). For the present work, the Sobol'
 251 based variance method was used (Sobol', 1993). This method allows evaluating the sensitivity
 252 of a model to interaction between input variables. It consists of numerous simulations of the
 253 models using two independent samples of N repetitions (rows) and k input variables
 254 (columns), retrieved from existing data or randomly generated data from the probability
 255 distribution function of each k input variable. One or several variables in the first sample are
 256 substituted by the same variable(s) taken from the second sample. For each of the (2^k-1)
 257 possible combinations of variable substitutions between the two samples, N runs of the model
 258 are computed. The sensitivity of the model to input variables is based on so-called sensitivity
 259 or Sobol' indices, which are calculated on the principle of the decomposition of the total
 260 variance V of the model output, in response to individual or simultaneous variations of the k
 261 model inputs:

$$262 \quad V = \sum_i V_i + \sum_{i<j} V_{ij} + \sum_{i<j<m} V_{ijm} + \dots + V_{1,2,\dots,k} \quad (13)$$

263 Where V_i is the model output variance in response to variation of the i th input variable, V_{ij} is
 264 the model output variance in response to the simultaneous variation of the i th and the j th
 265 model input, and so-on. Then, sensitivity indices are calculated as follows:

$$266 \quad S_i = \frac{V_i}{V} \quad (14)$$

$$267 \quad S_{Ti} = \frac{V_i + \sum_j V_{ij} + \sum_{j<m} V_{ijm} + \dots + V_{i,j,\dots,k}}{V} \quad (15)$$

268 where j and m are the j th and the m th model input variables, and $i \neq j \neq m$. S_i is called the first
 269 order sensitivity index. It measures the sensitivity of the model to the input variable X_i . S_{Ti} is
 270 called the total sensitivity index. It measures the impact of variations of the i th model input on
 271 the model output, including all the possible interactions with other input variations. For more
 272 details about the Sobol' method, see Saltelli (2002).
 273

274 2.4.2 Sensitivity analysis of *PM* reference evapotranspiration formula

275 A major constraint, when trying to perform a sensitivity analysis, is the interdependency of
 276 input variables. Considering the Penman-Monteith FAO-56 formula, required input data are
 277 minimum and maximum air temperature, minimum and maximum relative humidity, solar
 278 radiation and wind speed. Minimum and maximum air temperature and relative humidity, if
 279 picked randomly in a data set, will lead to nonsense computations, i.e. having a minimum air

280 temperature or relative humidity value higher than the maximum. To solve this problem
 281 average air temperature and relative humidity and their daily amplitudes were calculated prior
 282 to elaborating the two random data sets required for Sobol' method:

$$283 \quad T = \frac{T_{\min} + T_{\max}}{2} \quad ; \quad RH = \frac{RH_{\min} + RH_{\max}}{2} \quad (16) ; (17)$$

284 and

$$285 \quad \Delta T = T_{\max} - T_{\min} \quad ; \quad \Delta RH = RH_{\max} - RH_{\min} \quad (18) ; (19)$$

286 where T and RH are the daily average air temperature [°C] and the daily average relative
 287 humidity [%], ΔT [°C] and ΔRH [%] are their daily amplitude, and T_{\min} , T_{\max} , RH_{\min} and
 288 RH_{\max} having the signification and units as in equations (6) and (9). Once random samples are
 289 created, T , RH , ΔT and ΔRH are used to retrieve minimum and maximum air temperature and
 290 relative humidity daily values, inverting the equations (16), (17), (18) and (19).

291 A major requirement of sensitivity analysis is the choice of the input data set. The aim of the
 292 present SA is to retrieve the climate variables which PM model is most sensitive to, according
 293 to different climatic conditions, i.e. Oceanic and Mediterranean climates. It is assumed that
 294 the climate stations within both study areas (8 for SW and 11 for SE) provide a good sample
 295 of the spatial variation of climatic conditions. To take into account the variability of climate
 296 during the year, sensitivity analyses were performed for each month. That is, the input data set
 297 for Sobol' SA is generated for a given month, according to the probability distribution
 298 function (PDF) of each input data, recorded at the stations of a given study area (SW or SE).
 299 For each month and each area, Sobol' SA was assessed as follows (figure 2): (a) empirical
 300 PDF of each input variable were fitted to empirical distributions of the data sets recorded at
 301 the (8 or 11) climate stations area during 2000 to 2004, using a Gaussian Kernel fitting
 302 function with R statistical software (R Development Core Team, 2007) ; (b) Two samples
 303 were generated by quasi-random sampling with 10000 repetitions ; (c) Several model outputs
 304 and variance decomposition were computed using Sobol' algorithm of the package *sensitivity*
 305 of R statistical software ; (d) First order and total sensitivity indexes and their monthly
 306 evolution were then compared. Note that for step (b), one could propose the use of the
 307 original data record rather than random sample generations. However, the number of available
 308 data for each month was not sufficient for the statistical robustness of the analysis.

310 2.5 Statistical indices used for satellite sensed solar radiation and empirical E_0 formulae 311 evaluations

312 The reference data used to evaluate satellite-sensed solar radiation were pyranometer records
 313 at ground level. For evapotranspiration, PM (equation (1)), using pyranometer records, was
 314 used as a reference data for empirical formulae evaluation. For each day i , the difference
 315 between reference and estimated data was calculated as follows :

$$316 \quad D_i = Est_i - Ref_i \quad (20)$$

317 where D is the difference (or "error") [mm], Est_i is the satellite-sensed solar radiation or the
 318 E_0 estimated with an empirical method and Ref_i is the reference data. The units are MJ m⁻² or
 319 mm according to the type of data evaluated.

320 The accuracy of each method is given by the bias (or mean error):

$$321 \quad bias = \frac{1}{n} \sum_{i=1}^n D_i \quad (21)$$

322 The unit of $bias$ is mm or MJ m⁻², according to the type of data evaluated, and n is the number
 323 of days.

324 The precision is given by the root mean squared error (RMSE):

325

$$RMSE = \sqrt{\frac{1}{n} \sum_{i=1}^n D_i^2} \quad (25)$$

326

Errors populations were also analyzed by means of coefficient of determination (R^2).

327

328 **3 Results and discussion**

329 *3.1 Sensitivity analysis of PM formula*

330 *Sensitivity of E_0 computation using PM method in Southwest area (Oceanic climate).* The
331 results of monthly sensitivity analyses computed using Southwest area data show clear
332 seasonal trends (figure 3A). During the winter period (from November to February), wind
333 speed is the main source of variation in E_0 values calculated using *PM* method (e.g. 38% of E_0
334 total variance in January, table 2). Then come relative humidity and air temperature (32% and
335 17% of E_0 total variance in January, respectively). Solar radiation, daily amplitude of air
336 temperature and daily amplitude of relative humidity have little impact on evapotranspiration
337 process during winter. This trend changes during March and October. From April to
338 September, E_0 is mostly sensitive to solar radiation (up to 74% of E_0 total variance in May,
339 and 70% in July). From May to July, *PM* formula is not very sensitive to *RH*, U_2 , ΔRH and
340 ΔT . Mean daily air temperature participate from 11% to 15% of E_0 variance, from May to
341 September. Total sensitivity indices show that, when added to other variables variations, air
342 temperature has a greater impact on E_0 variability during summer, and wind speed has a
343 greater impact during winter (figure 3B).

344 *Sensitivity of E_0 computation using PM method in Southeast area (Mediterranean climate).*

345 The sensitivity of *PM* formula to climate input variables in Mediterranean climate conditions
346 is very close to the one observed for Oceanic climate. Wind speed as a major impact on E_0
347 calculation during winter and solar radiation is clearly the most influent variable during
348 summer (figures 3C and 3D, table 2).

349 The present analysis highlights the great sensitivity of this Penman-Monteith formula to solar
350 radiation during summer period, when E_0 reaches its highest values, and when its calculation
351 is critical for irrigation process and ecological modelling. These results were obtained for
352 Mediterranean and Oceanic climate, at medium latitudes. They are consistent with former
353 uncertainty and sensitivity analyses performed in Mediterranean climate (Llasat and Snyder,
354 1998 ; Rana and Katerji, 1998). A recent work published by Gong et al. (2006) on a large
355 range of climatic conditions in Southern China leads to similar results, except for relative
356 humidity which had a greater impact on E_0 during winter than it has been shown in the
357 present study.

358 Considering the results of Penman-Monteith sensitivity to solar radiation, it seems reasonable
359 to evaluate the benefits of satellite sensed solar radiation to E_0 calculation when no solar
360 radiation ground records are available. This point is studied and discussed in the next section.

361

362 *3.2 Remotely sensed solar radiation performances*

363 Table 3 shows the annual error statistics of solar radiation and E_0 data calculated with
364 HelioClim-1 data instead of pyranometer radiation data. HelioClim-1 underestimates daily
365 irradiation (figures 4A and 4D). The bias is twice as important for Southwest area (-
366 1.87 MJ m⁻²) as it is for Southeast area (-1.07 MJ m⁻²). RMSE is also higher for SW (20% of
367 the annual solar irradiation) than for SE (14%). Although the uncertainty, in absolute value, is
368 larger during summer period (Figure 5A), the RMSE are 15% (SW) and 10% (SE) of R_S
369 pyranometer value in July, whereas they reach 26% (SW) and 18% (SE) in January, as
370 irradiation is larger during summer.

371 These errors are consistent with those observed in Northern Europe, during former
372 evaluations of HelioClim-1 database (Lefèvre *et al.*, 2007). When no pyranometer data is

373 available, daily satellite sensed solar radiation should be preferred to temperature-based
374 estimations: for both areas, daily irradiation RMSE are 3 to 4 times smaller than those
375 obtained by Hunt *et al.* (2000) in Ontario (Canada), with empirical formulae based on air
376 temperature. Moreover, HelioClim-1 irradiation may be as precise as pyranometer
377 measurements where weather stations are not steadily maintained or not equipped with
378 accurate devices: uncertainty reported varies from 5 to 25%, according to the class of material
379 and the metrology experts (Llasat and Snyder, 1998 ; Droogers and Allen, 2002).
380 There are several sources of uncertainties when comparing satellite data to very local
381 measurements, such as weather station records. This point has been widely discussed by
382 Zelenka *et al.* (1999). First, it is difficult to compare pixel data, corresponding to a surface,
383 with a discrete measurement, such as pyranometer weather station records. Another category
384 of uncertainties comes from the spatial (1 pixel each 30 kilometer) and temporal (3 hours)
385 resolutions of the initial data set used to create the HelioClim-1 database. In addition, the
386 spatial interpolation method generates its intrinsic uncertainties. The Heliosat-2 method itself,
387 used to elaborate the HelioClim-1 database, also participate to uncertainties of satellite sensed
388 irradiation data (e.g. the algorithm limits). The uncertainties inherent to the ISCCP-B2 data
389 set could be avoided by applying the Heliosat-2 method to each original Meteosat pixel and
390 for every hour. The HelioClim-2 database was created in that respect but begins only in 2004
391 and could not be used in this study.

392

393 3.3 Propagation of satellite sensed solar radiation errors in E_0 formulae

394 Replacing pyranometer measurement by Heliosat-2 estimations (*i.e.* HelioClim-1 data)
395 induces little error for reference evapotranspiration calculation using the Penman-Monteith
396 model (table 3). Estimation errors are higher for middle range E_0 values (figure 4B and 4E).
397 This could be explained by the fact that most of the errors occur for partially cloudy days, due
398 to uncertainties in retrieving daily solar radiation with Heliosat-2 method for this type of
399 weather (Rigollier *et al.*, 2004). In both areas, E_{PM} is slightly underestimated. For SW, biases
400 vary from -0.34 mm to 0.01 mm, according to the season (figure 5B). The annual RMSE
401 value remains low (11% of E_0 mean value). In SE area, E_{PM} bias is negligible (-0.20 mm to
402 0.01 mm, figure 5C). Relative RMSE in SE is 7% of E_0 mean value, which is lower than in
403 SW. Heliosat-2 method is more successful for clear sky days, which could explain the
404 difference between the two regions, as clear sky situations occur more frequently in SE than
405 SW. Relative errors of E_{PM} calculated with HelioClim-1 are lower during summer (9% for
406 SW and 5% for SE, in July). Again, the better performance of Heliosat-2 method for clear sky
407 days could explain this seasonal trend, as clear sky situations are more numerous during
408 summer than during the other seasons. Yet, higher relative errors could have been expected:
409 sensitivity analyses have shown that solar radiation has the greatest impact on PM model
410 during summer (*i.e.* when evapotranspiration reaches its maximum) in Oceanic or
411 Mediterranean climates (see section 3.1).

412 Errors are higher when pyranometer data is replaced by HelioClim-1 data in radiation
413 methods, *i.e.* HR , TU and PT (figure 4C and 4F, table 3). Biases are mostly negative.
414 Sensitivity to solar radiation errors is higher for radiation methods than for PM because
415 radiation methods do not include advective effects on the evapotranspiration process and thus
416 are mainly governed by radiative transfers. The largest error propagation can be observed for
417 the Hargreaves radiation method (table 3, figures 5B and 5C).

418

419 3.4 Empirical formulae performance

420 Daily E_0 values of 4 empirical methods were compared to reference evapotranspiration
421 computed with PM . HelioClim-1 solar radiation was used for radiation methods, whereas

422 pyranometer data was used for *PM*, as it was considered here as the “control” method. Data
423 sources used for E_0 calculations are shown in table 4.
424 In both areas, Hargreaves temperature method (*HT*) gave the highest uncertainties for the
425 annual period (table 5). During summer, formulae using satellite-sensed solar radiation
426 improve considerably E_0 estimation compared to *HT* estimates based solely on local air
427 temperature. Figures 6A and 6B show an obvious seasonal trend of *HT* errors, which is
428 related to the variations in sensitivity of E_0 to the different input variables of *PM*: during
429 summer, when E_0 is mainly governed by solar radiation, estimates based upon air temperature
430 only are thus less accurate.
431 Evapotranspiration calculated with satellite-sensed solar radiation is mainly underestimated.
432 For both climates, all radiation methods show biases similar to those induced by replacement
433 of pyranometer data by satellite-sensed solar radiation (between -0.4 mm and -0.2 mm, table 3
434 and 5): this suggests that the underestimation observed is mainly due to the propagation of
435 HelioClim-1 data bias within radiation methods, rather than wrong calibration of empirical
436 coefficients used in these formulae.
437 In the Southwest area, *PT* data is strongly correlated to *PM* data ($R^2 = 0.938$, table 5). It is
438 also the formula providing the lowest E_0 RMSE during summer and for the whole year (figure
439 6A). Turc and Hargreaves radiation method performances are almost the same. The
440 performance of *TU* is slightly better than other formulae from September to November. It has
441 been shown in former studies that the Turc method provides good results in humid
442 environment (Jensen et al., 1990 ; Turc, 1961), whereas Hargreaves radiation method has
443 been established from arid or semi-arid climate data analysis (Hargreaves and Allen, 2003).
444 These differences between those two formulae did not emerge from the current study, in
445 Southwest oceanic climate. Hargreaves temperature method provided the lowest RMSE and
446 the lowest bias (in absolute value), from January to April. However, this temperature-based
447 method was the least accurate method for SW, when considering summer and annual periods
448 (RMSE = 0.67 mm, $R^2=0.894$, for the whole year). *HT* overestimated E_0 (a mean error of
449 0.32 mm).
450 For the Southeast area, all empirical formulae showed poorer performances when compared to
451 the Southwest region (figure 6B). The higher wind speed and the lower relative humidity in
452 SW throughout the year might explain these differences (results not shown). *HR* provided the
453 most precise E_0 estimates for the whole year (RMSE= 0.77 mm, i.e. 25% of E_0 mean annual
454 value). The best correlation with *PM* values is provided by *PT*. The Priestley-Taylor formula
455 performed better than every other formula during summer, but showed considerable bias and
456 RMSE during winter. The lowest bias (in absolute value) is provided by *HT*, which showed in
457 contrast high RMSE (0.96 mm, i.e. 31% of the annual mean).
458 These results suggest that using satellite sensed-solar radiation within empirical formulae
459 improve the accuracy of E_0 estimates during summer and for the whole year, although
460 reference evapotranspiration remains underestimated in most cases.

462 **4 Conclusions**

463 The present work focused on the role of solar radiation data in reference evapotranspiration
464 calculation at daily time steps. A sensitivity analysis of the Penman-Monteith model showed
465 that solar radiation strongly governs reference evapotranspiration during summer, for Oceanic
466 and Mediterranean climates at medium latitude. The use of satellite-sensed solar radiation
467 taken from HelioClim-1 database for E_0 calculation was evaluated. It was shown that
468 HelioClim-1 data underestimates solar radiation at daily time step, for Oceanic and
469 Mediterranean climates in France. The RMSE ranges from 14 to 20% of the annual solar
470 radiation. The error propagation is considerable in radiation-based methods, as these
471 equations are linearly linked to solar radiation input.

472 Amongst the numerous studies concerning reference evapotranspiration estimates with
473 limited climatic data, few considered daily time step. When temperature data is the sole
474 climate variable available, Hargreaves temperature method is often used or recommended and
475 provides relative RMSE ranging from 20% to 30% of the mean annual value, depending on
476 the type of climate (Droogers and Allen, 2002 ; Hargreaves and Allen, 2003). In the present
477 work, we found that using satellite sensed global radiation via *PT* or *HR* methods improves E_0
478 estimates, compared to Hargreaves temperature method. With these empirical solar radiation-
479 based methods, relative annual RMSE ranges from 22% to 28 %, according to the method and
480 the type of climate, humid-Oceanic or semi-arid-Mediterranean. Hargreaves temperature
481 method, however, produced annual RMSE of 28% of the annual mean for Oceanic climate
482 and 31% for Mediterranean climate. The difference in precision between radiation and
483 Hargreaves temperature method reaches its maximum during summer, when the E_0 process is
484 mainly governed by solar radiation. In contrast, *HT* showed smaller uncertainties than
485 radiation methods with HelioClim-1 data during winter.
486 These results suggest that during summer, using empirical radiation methods with satellite
487 sensed solar radiation from the HelioClim-1 database to estimate E_0 should be preferred to
488 *HT*, when air temperature is the only available record at weather stations.
489 These observations need to be verified in other climatic conditions, and especially in arid
490 climates, where E_0 estimation is crucial for water management. This could be easily done
491 using HelioClim-1 database, as it provides data for a large surface of the globe, i.e. from
492 Northern Europe to South-Africa.

493

494 **Acknowledgements**

495 The authors would like to thank the Conseil Interprofessionnel des Vins de Bordeaux for their
496 financial and technical support. Thanks to the Center for Energy and Processes (Centre
497 Energétique et Procédés, Sophia-Antipolis, France) for providing HelioClim-1 data.

498 **References**

- 499 Allen, R.G., Jensen, M.E., Wright, J.L. and Burman, R.D., 1989. Operational estimates of
500 reference evapotranspiration. *Agronomy Journal*, 81(4): 650-662.
- 501 Allen, R.G., Pereira, L.S., Raes, D. and Smith, M., 1998. Crop evapotranspiration: guidelines
502 for computing crop water requirements. FAO Irrigation and Drainage Paper. Food and
503 Agriculture Organization (FAO), Rome Italy, 300 pp.
- 504 Bois, B., Pieri, P., Van Leeuwen, C. and Gaudillere, J.P., 2005. Sensitivity analysis of the
505 Penman-Monteith evapotranspiration formula and comparison of empirical methods
506 used in viticulture soil water balance, XIV International GESCO Viticulture Congress,
507 Geisenheim, Germany, 23-27 August, 2005.
- 508 Brisson, N., Seguin, B. and Bertuzzi, P., 1992. Agrometeorological soil water balance for
509 crop simulation models. *Agricultural and Forest Meteorology*, 59(3-4): 267-287.
- 510 Cano, D., Monget, J.-M., Albuissou, M., Guillard, H., Regas, N. and Wald L., 1986. A
511 method for the determination of the global solar radiation from meteorological
512 satellites data. *Solar Energy*, 37(1): 31-39.
- 513 Cukier, R.I., Levine, H.B. and Shuler, K.E., 1978. Nonlinear sensitivity analysis of
514 multiparameter model systems. *Journal of Computational Physics*, 26(1): 1-42.
- 515 Choudhury, B.J., 1997. Global pattern of potential evaporation calculated from the Penman-
516 Monteith equation using satellite and assimilated data. *Remote Sensing of*
517 *Environment*, 61(1): 64-81.
- 518 Droogers, P. and Allen, R.G., 2002. Estimating reference evapotranspiration under inaccurate
519 data conditions. *Irrigation and Drainage Systems*, 16(1): 33-45.
- 520 Fisher, J.B., DeBiase, T.A., Qi, Y., Xu, M. and Goldstein, A.H., 2005. Evapotranspiration
521 models compared on a Sierra Nevada forest ecosystem. *Environmental Modelling &*
522 *Software*, 20(6): 783-796.
- 523 Frey, H.C. and Patil, S.R., 2002. Identification and review of sensitivity analysis methods.
524 *Risk Analysis*, 22(3): 553-578.
- 525 Garcia, M., Raes, D., Allen, R. and Herbas, C., 2004. Dynamics of reference
526 evapotranspiration in the Bolivian highlands (Altiplano). *Agricultural and Forest*
527 *Meteorology*, 125(1/2): 67-82.
- 528 Gavilan, P., Lorite, I.J., Tornero, S. and Berengena, J., 2006. Regional calibration of
529 Hargreaves equation for estimating reference ET in a semiarid environment.
530 *Agricultural Water Management*, 81(3): 257-281.
- 531 Gong, L., Xu, C.-y., Chen, D., Halldin, S. and Chen, Y.D., 2006. Sensitivity of the Penman-
532 Monteith reference evapotranspiration to key climatic variables in the Changjiang
533 (Yangtze River) basin. *Journal of Hydrology*, 329(3/4): 620-629.
- 534 Guyot, G., 1997. *Climatologie de l'environnement. De la plante aux écosystèmes*. Masson,
535 Paris, 505 pp.
- 536 Hargreaves, G.H. and Allen, R.G., 2003. History and Evaluation of Hargreaves
537 Evapotranspiration Equation. *Journal of Irrigation and Drainage Engineering*, 129(1):
538 53-63.
- 539 Hargreaves, G.H. and Samani, Z.A., 1982. Estimating Potential Evapotranspiration. *Journal*
540 *of the Irrigation and Drainage Division*, 108: 223-230.
- 541 Hargreaves, G.L., Hargreaves, G.H. and Riley, J.P., 1985. Agricultural benefits for Senegal
542 River Basin. *Journal of Irrigation and Drainage Engineering*, 111: 111-124.
- 543 Hunt, L. A., Kuchar, L. and Swanton, C. J., 1998. Estimation of solar radiation for use in crop
544 modelling. *Agricultural and Forest Meteorology* 91 (3/4): 293-300.
- 545 Jensen, M.E., Burman, R.D. and Allen, R.G., 1990. Evapotranspiration and Irrigation Water
546 Requirements. *ASCE Manuals and Reports on Engineering Practices*, 70. American
547 Society of Civil Engineers, New York, 360 pp.

548 Lebon, E., Dumas, V., Pieri, P. and Schultz, H.R., 2003. Modelling the seasonal dynamics of
549 the soil water balance of vineyards. *Functional Plant Biology*, 30(6): 699-710.

550 Lefèvre, M., Remund, J., Albuissou, M. and Wald, L., 2002. Study of effective distances for
551 interpolation schemes in meteorology. *Geophysical Research Abstracts*, 4, April 2002,
552 EGS02-A-03429, European Geophysical Society.

553 Lefevre, M., Wald, L. and Diabate, L., 2007. Using reduced data sets ISCCP-B2 from the
554 Meteosat satellites to assess surface solar irradiance. *Solar Energy*, 81(2): 240-253.

555 Llasat, M.C. and Snyder, R.L., 1998. Data error effects on net radiation and
556 evapotranspiration estimation. *Agricultural and Forest Meteorology*, 91(3/4): 209-221.

557 Monteith, J.L., 1981. Evaporation and surface temperature. *Quarterly Journal Of The Royal*
558 *Meteorological Society*, 107(451): 1-27.

559 Penman, H.L., 1948. Natural evaporation from open water, bare soil and grass. *Proceedings of*
560 *the Royal Society of London*, A193: 120-146.

561 Pereira, A.R., 2004. The Priestley-Taylor parameter and the decoupling factor for estimating
562 reference evapotranspiration. *Agricultural and Forest Meteorology*, 125(3/4): 305-313.

563 Pereira, A.R. and Pruitt, W.O., 2004. Adaptation of the Thornthwaite scheme for estimating
564 daily reference evapotranspiration. *Agricultural Water Management*, 66(3): 251-257.

565 Popova, Z., Kercheva, M. and Pereira, L.S., 2005. Validation of the FAO methodology for
566 computing ET₀ with limited data, ICID 21st European Regional Conference,
567 Frankfurt and Slubice, 13pp.

568 Priestley, C.H.B. and Taylor, R.J., 1972. On assessment of surface heat flux and evaporation
569 using large-scale parameters. *Monthly Weather Review*, 100: 81-92.

570 R Development Core Team, 2007. R: A Language and Environment for Statistical
571 Computing. R Foundation for Statistical Computing, Vienna, Austria.

572 Rigollier, C., Bauer, O. and Wald, L., 2000. On the clear sky model of the ESRA - European
573 Solar Radiation Atlas - With respect to the Heliosat method. *Solar Energy*, 68(1): 33-
574 48.

575 Rigollier, C., Lefevre, M. and Wald, L., 2004. The method Heliosat-2 for deriving shortwave
576 solar radiation from satellite images. *Solar Energy*, 77(2): 159-169.

577 Rana, G. and Katerji, N., 1998. A Measurement Based Sensitivity Analysis of the Penman-
578 Monteith Actual Evapotranspiration Model for Crops of Different Height and in
579 Contrasting Water Status. *Theoretical and Applied Climatology*, 60(1): 141-149.

580 Saltelli, A., 2002. Making best use of model evaluations to compute sensitivity indices.
581 *Computer Physics Communications*, 145(2): 280-297.

582 Saltelli, A., Ratto, M., Tarantola, S. and Campolongo, F., 2006. Sensitivity analysis practices:
583 Strategies for model-based inference. *Reliability Engineering & System Safety*, 91(10-
584 11): 1109-1125.

585 Sobol', I.M., 1993. Sensitivity analysis for non-linear mathematical model. *Mathematical*
586 *Modeling and Computational Experiment*, 1: 407-414.

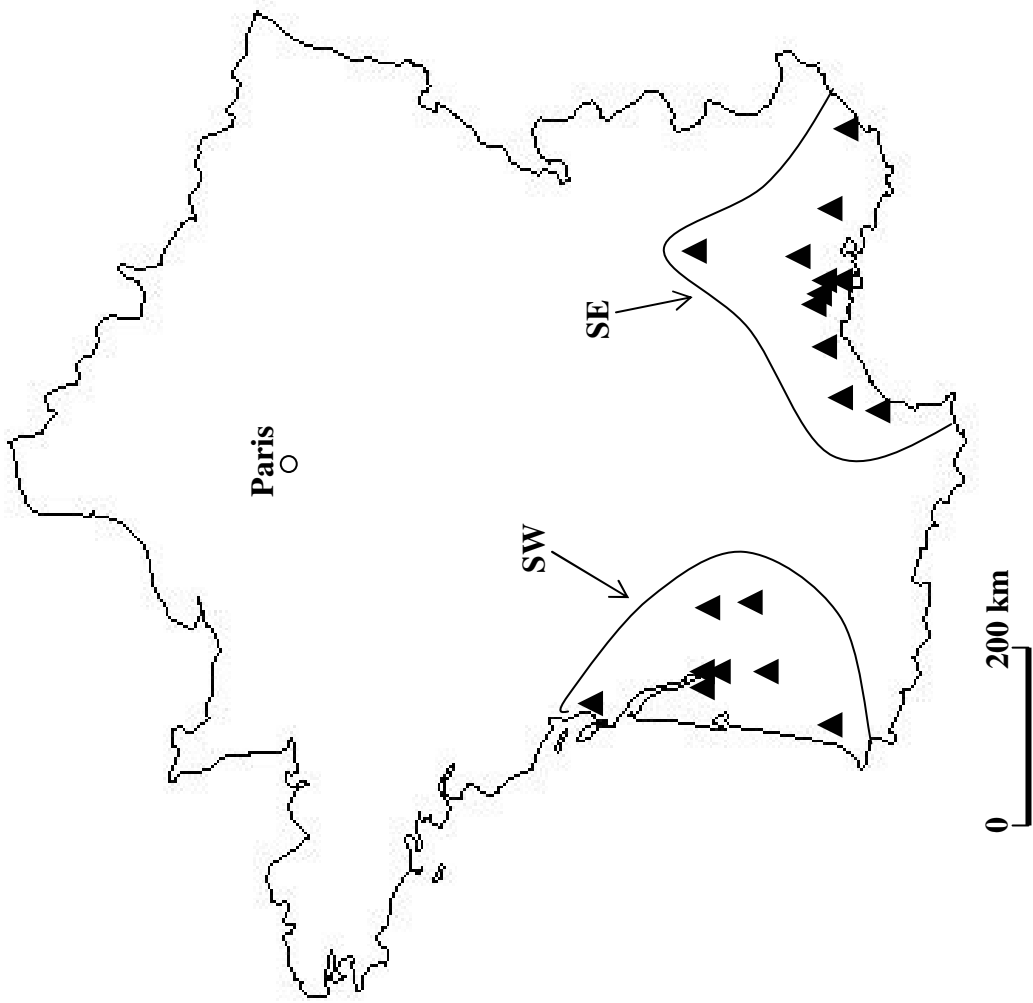
587 Struzik, P., 2001. Spatialisation of Solar Radiation - draft report on possibilities and
588 limitations, COST action 718, 3rd Management committee and Working Group
589 Meeting, Budapest, Hungary, pp. 12.

590 Turc, L., 1961. Evaluation des besoins en eau d'irrigation, évapotranspiration potentielle.
591 *Annales Agronomiques*, 12(1): 13-49.

592 Xu, C.Y. and Singh, V.P., 2000. Evaluation and generalization of radiation-based methods for
593 calculating evaporation. *Hydrological Processes*, 14: 339-349.

594 Xu, C.Y. and Singh, V.P., 2002. Cross comparison of empirical equations for calculating
595 potential evapotranspiration with data from Switzerland. *Water Resources*
596 *Management*, 16(3): 197-219

597 Zelenka, A., Perez, R., Seals, R. and Renne, D., 1999. Effective accuracy of satellite-derived
598 hourly irradiances. *Theoretical and Applied Climatology*, 62(3/4): 199-207.
599
600 SoDa web site: <http://www.soda-is.org>
601



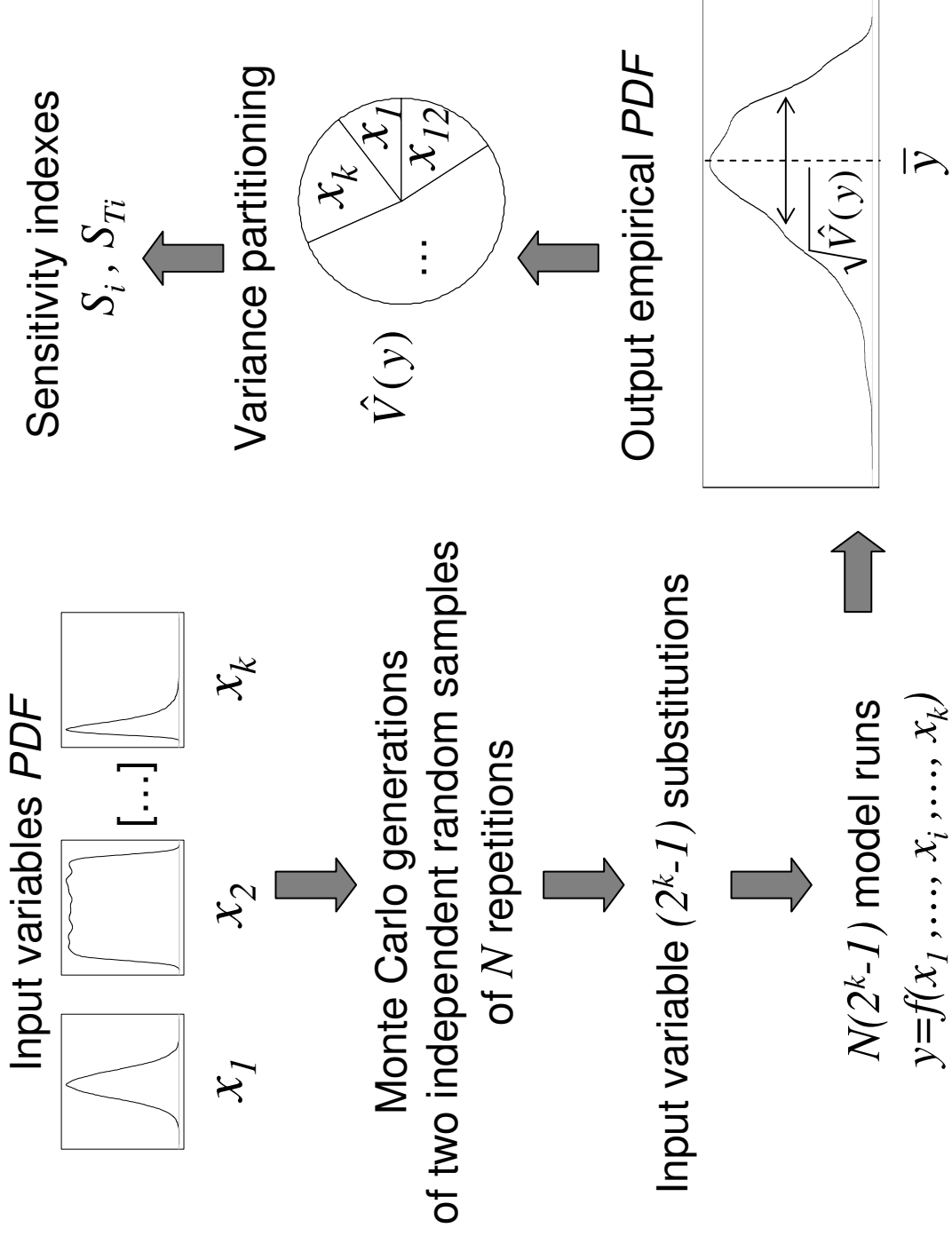
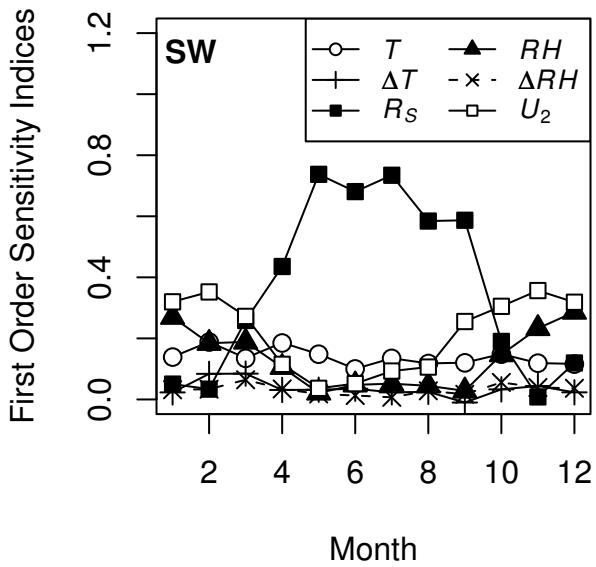
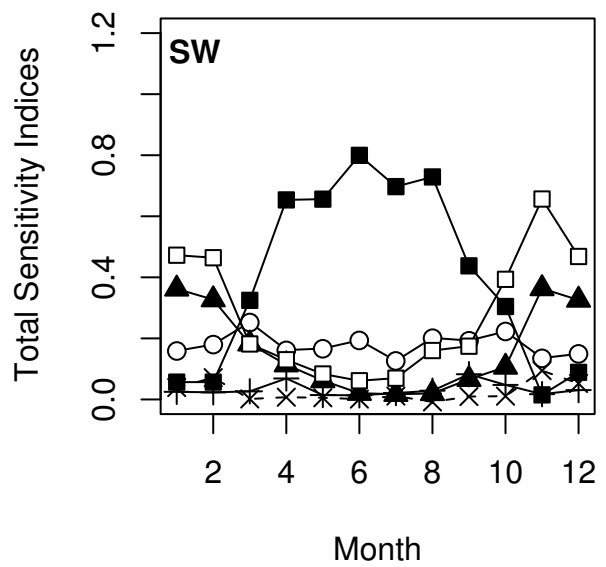


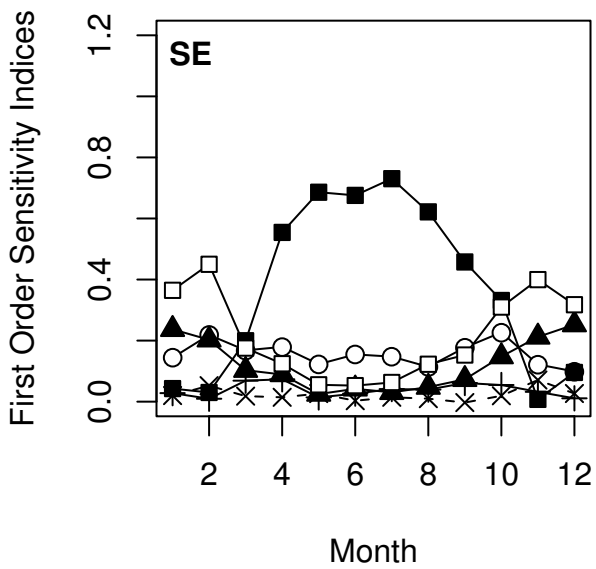
Fig 3. SA monthly indices



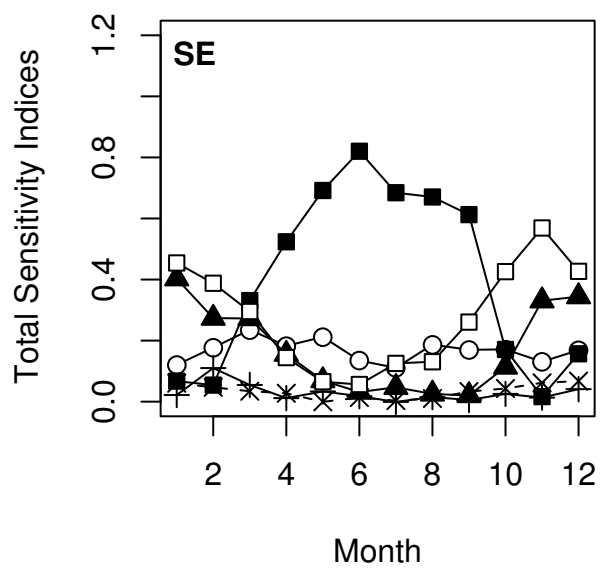
A



B



C



D

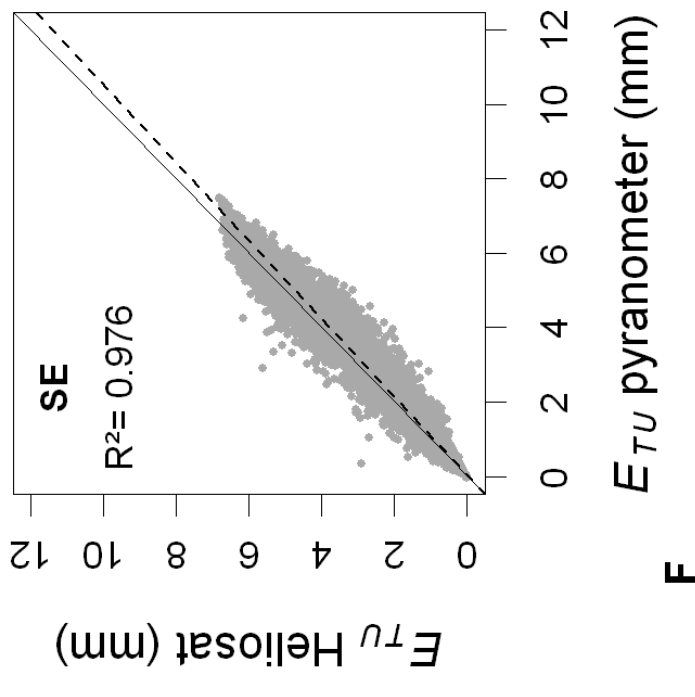
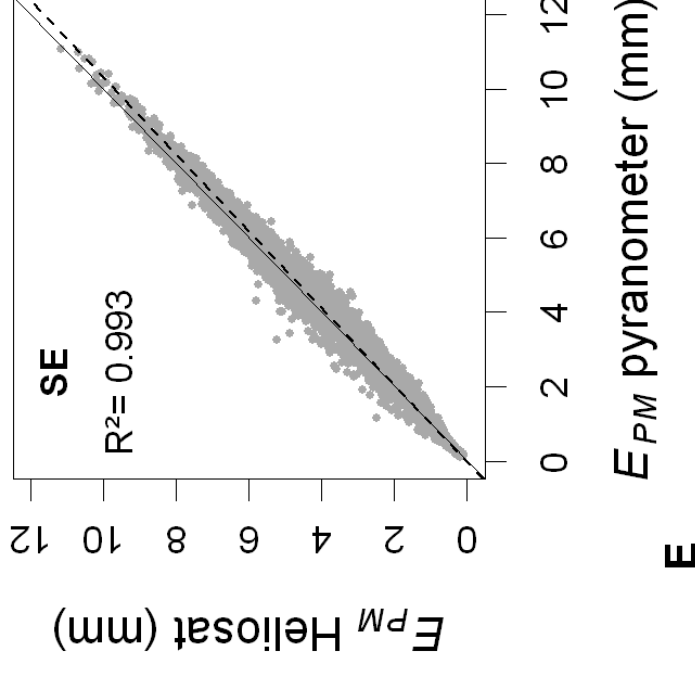
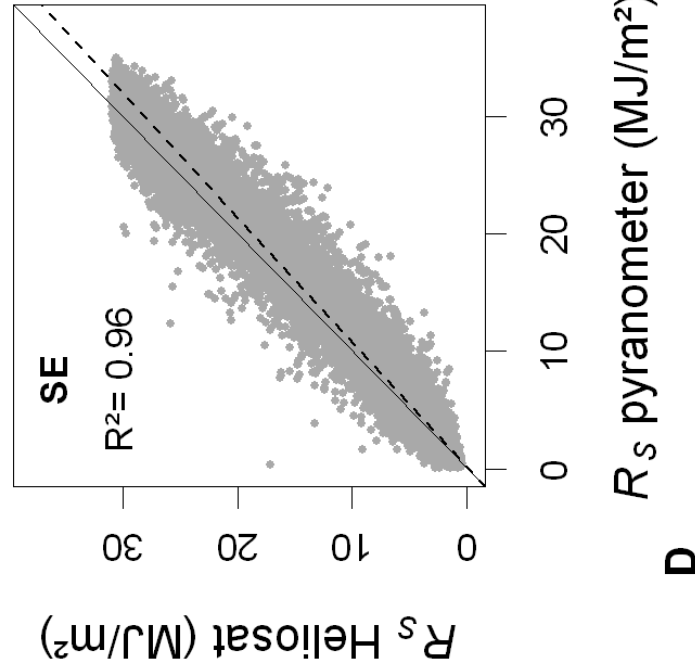
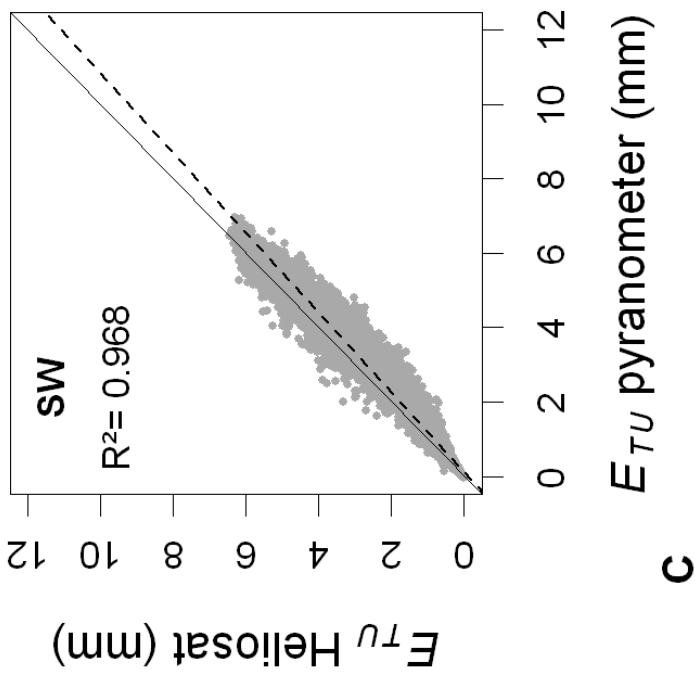
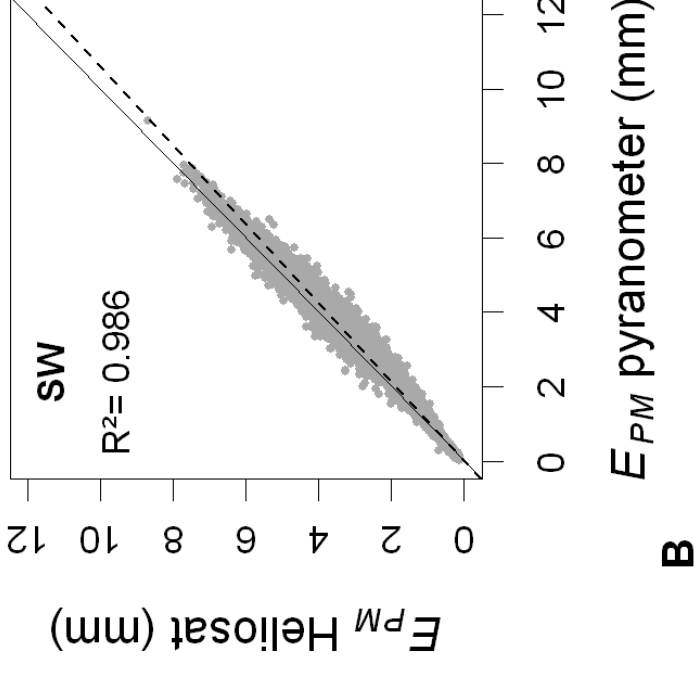
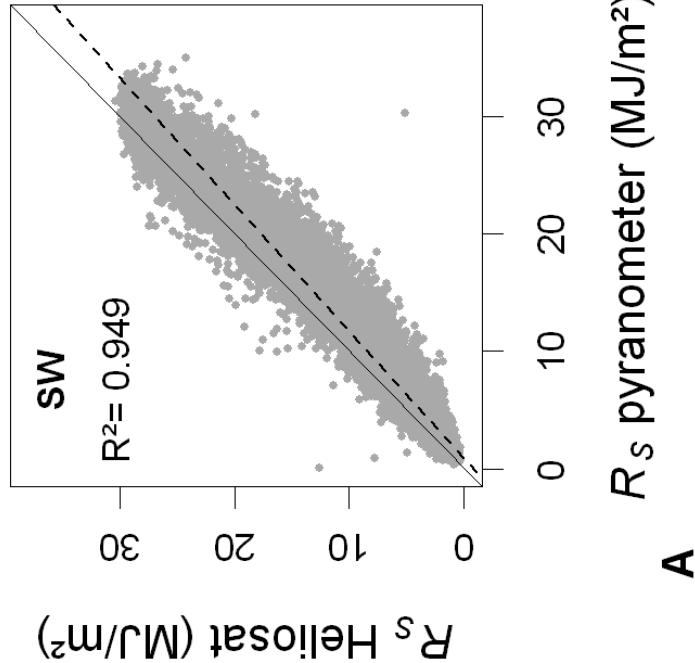


Fig 5. RMSE induced using Helioclim data by month

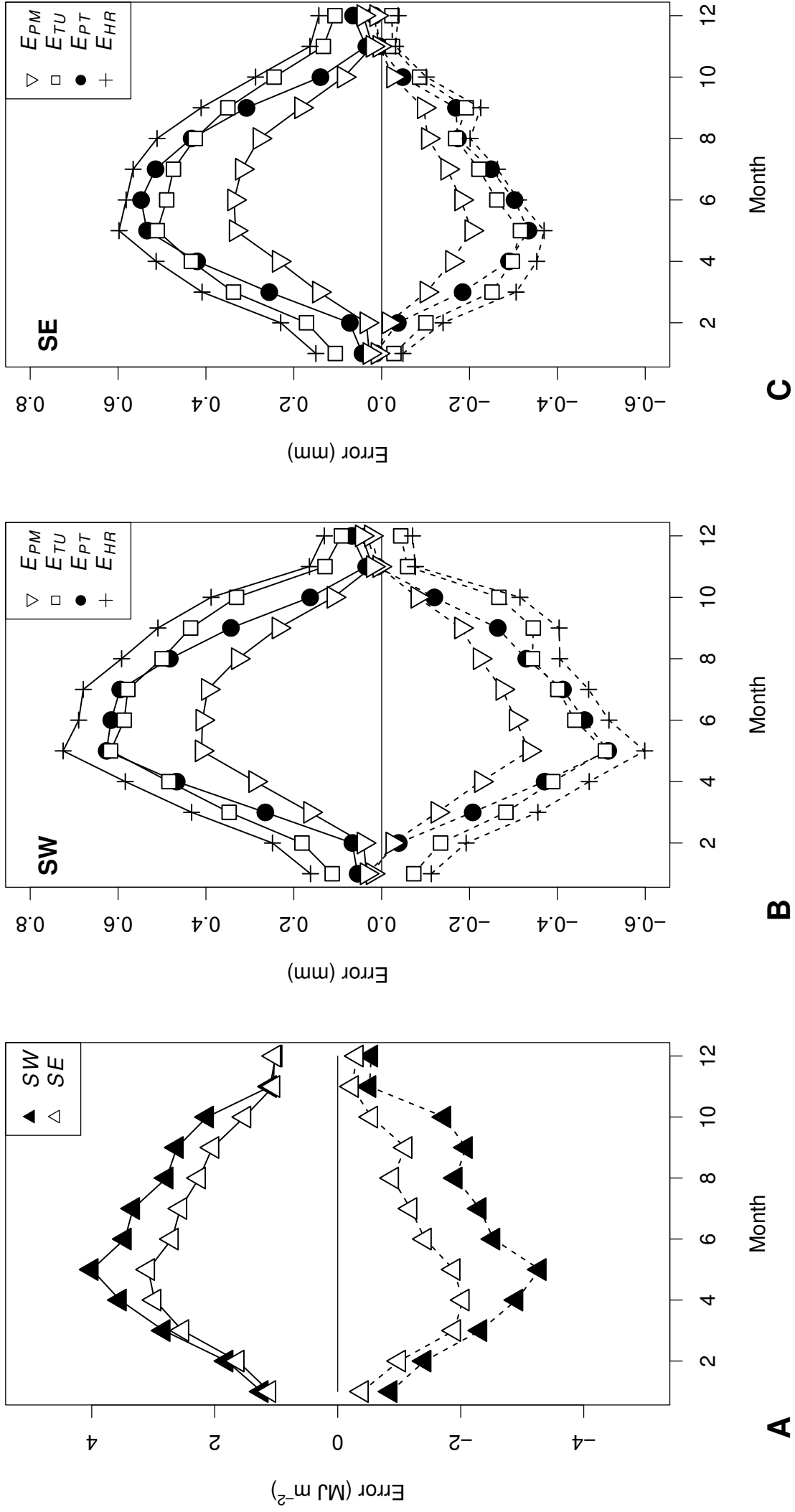


Fig 6. RMSE of empirical formulae by month

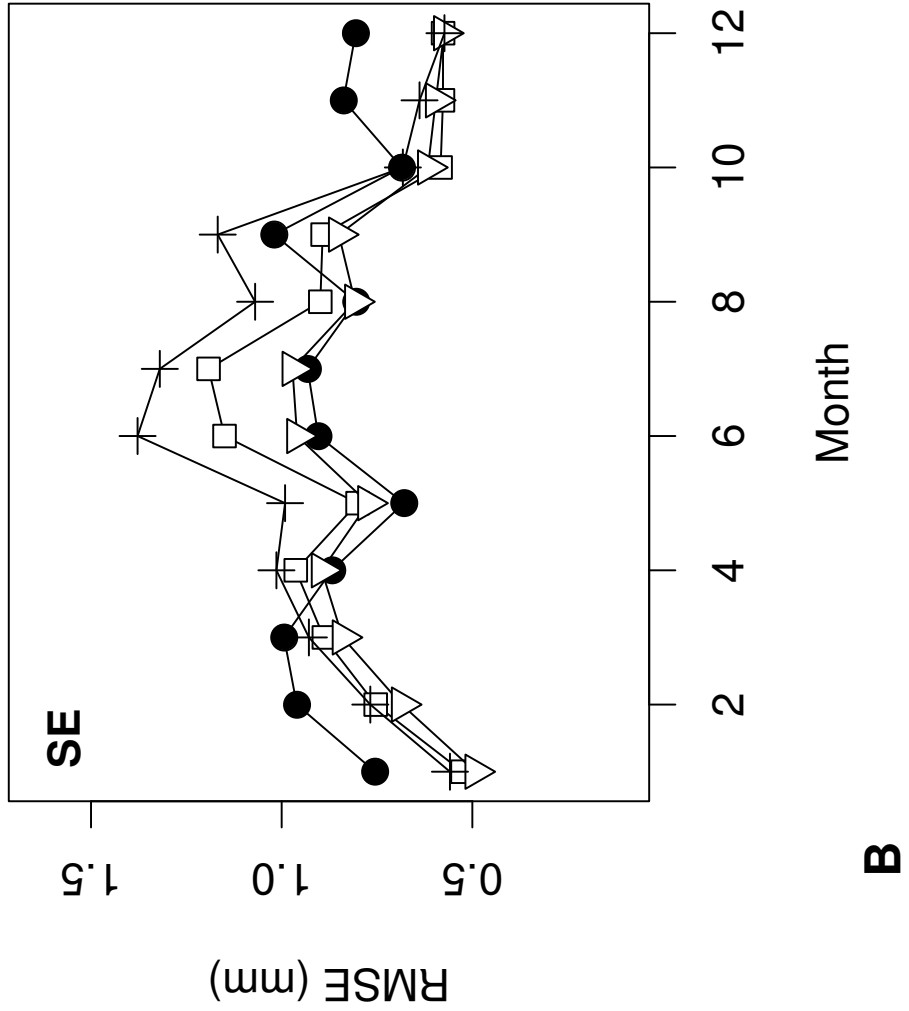
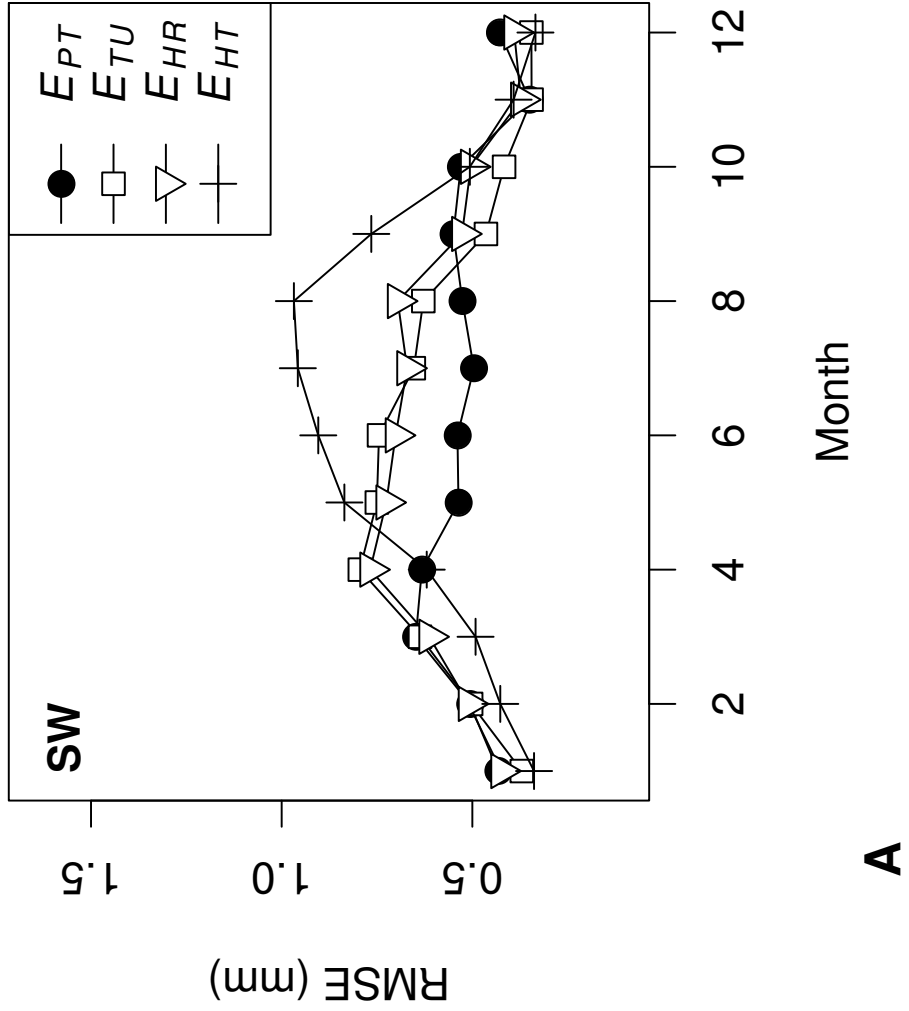


Figure captions

Fig. 1. Spatial distribution of the 19 meteorological stations used in the study. SW: Southwest area, SE: Southeast area.

Fig. 2. General scheme of Sobol' sensitivity analysis. *PDF* = Probability Distribution Function. x_i = the *i*th variable of the model's *k* input variables. *y* = the model output.

Fig. 3. Monthly variations of first order and total sensitivity indices of climate input variables of *PM* model, for reference evapotranspiration calculation. **A** and **B**: Southwest area (SW) ; **C** and **D**: Southeast area (SE).

Fig. 4. Scatter plots of pyranometer and HelioClim-1 data. **A, B, C**: Southwest area (SW). **D, E, F**: Southeast area (SE). R_s : daily solar irradiation ; E_{PM} : E_0 daily value with Penman-Monteith (*PM*) method ; E_{TU} : E_0 daily value with Turc (*TU*) method. —: (1:1) curve ; ----: linear fitting curve.

Fig. 5. Errors induced by the use of daily HelioClim-1 data for irradiation (**A**), and E_0 estimates (**B**: Southwest area, **C**: Southeast area). *PM*: Penman-Monteith, *PT*: Priestley-Taylor, *TU*: Turc, *HR*: Hargreaves radiation, *HT*: Hargreaves temperature. : RMSE ; ----: Bias.

Fig. 6. Monthly variations of RMSE resulting from the comparison of daily E_0 between Penman-Monteith and estimation formulae (*PT*: Priestley-Taylor, *TU*: Turc, *HR*: Hargreaves radiation, *HT*: Hargreaves temperature). **A**: Southwest area ; **B**: Southeast area.

Table 1
List of weather stations used in the study

# code	Site	Latitude N (°)	Longitude W (°)	Elevation (m)	Mean E_0 (mm d ⁻¹) ^a	N ^b
South West						
1	BERGERAC	44.855	-0.521	33	2.34	1783
2	BOURRAN	44.334	-0.413	60	2.43	1606
3	CADAUJAC	44.753	0.554	20	2.36	1827
4	LATRESNE	44.780	0.478	63	2.54	1826
5	LUXEY	44.226	0.491	101	2.30	1818
6	SAINTE LAURENT-DE-LA-PREE	45.990	1.033	3	2.46	1827
7	SAINTE MARTIN DE HINX	43.576	1.269	64	2.29	1826
8	VILLENAVE D'ORNON	44.789	0.578	25	2.55	1827
South East						
1	AVIGNON	43.916	-4.876	24	3.27	1827
2	BELLE GARDE	43.781	-4.477	61	3.15	1762
3	FOURQUES	43.692	-4.595	3	3.41	1826
4	FREJUS	43.434	-6.717	3	3.13	1827
5	GRUISSAN	43.137	-3.121	40	3.04	1827
6	LES-SAINTE-MARIES-DE-LA-MER	43.580	-4.499	1	3.23	1827
7	MONTPELLIER	43.647	-3.874	50	2.60	1613
8	ROUJAN	43.491	-3.321	78	2.45	774
9	SAINTE-MARCEL-LES-VALENCE	44.977	-4.930	190	2.97	1827
10	SAINTE-GILLES	43.714	-4.412	72	3.15	1775
11	SALON DE PROVENCE	43.646	-5.014	68	3.27	1604

^a E_0 was calculated with Penman-Monteith model (*i.e.* PM).

^b Number of available E_0 values (days) on the period 2000-2004. Maximum is 1827. Lower N values means that data used to calculate E_0 with Penman-Monteith model (*i.e.* temperature, relative humidity, wind speed or solar radiation) were unavailable on certain days.

Table 2

First order sensitivity indices of *PM* method to climate variables. The values between brackets correspond to the relative part of total E_0 variance explained by each input variable. Figures in bold correspond to the highest sensitivity index of each month.

	Month	T	ΔT	R_s	RH	ΔRH	U_2
South-West	January	0.14 (17%)	0.02 (3%)	0.05 (6%)	0.27 (32%)	0.03 (4%)	0.32 (38%)
	April	0.19 (20%)	0.03 (3%)	0.44 (48%)	0.11 (12%)	0.03 (4%)	0.12 (13%)
	July	0.13 (13%)	0.02 (2%)	0.73 (70%)	0.05 (5%)	0.01 (1%)	0.09 (9%)
South-East	January	0.14 (17%)	0.03 (3%)	0.04 (5%)	0.24 (28%)	0.02 (2%)	0.36 (44%)
	April	0.18 (17%)	0.07 (7%)	0.55 (54%)	0.09 (9%)	0.01 (1%)	0.12 (12%)
	July	0.15 (14%)	0.04 (4%)	0.73 (71%)	0.03 (3%)	0.01 (1%)	0.06 (6%)

Table 3

Bias and RMSE resulting from the use of Helioclim-1 data instead of pyranometer data for daily solar irradiation and daily E_0 estimates, using Penman-Monteith or radiation methods. Values between brackets are the ratio of the statistical index with the mean reference value (pyranometer solar radiation, and evapotranspiration calculated with pyranometer data).

	South-West				South-East			
	Mean	Bias	RMSE	N ^a	Mean	Bias	RMSE	N ^a
R_S (MJ m ⁻²)	13.48	-1.87 (-14%)	2.67 (20%)	14566	15.83	-1.07 (-7%)	2.16 (14%)	18997
E_{PM} (mm)	2.41	-0.14 (-6%)	0.25 (11%)	14308	3.10	-0.08 (-3%)	0.21 (7%)	18448
E_{TU} (mm)	2.38	-0.27 (-11%)	0.41 (17%)	14308	2.87	-0.16 (-6%)	0.35 (12%)	18448
E_{PT} (mm)	2.34	-0.22 (-9%)	0.39 (17%)	14308	2.77	-0.14 (-5%)	0.34 (12%)	18448
E_{HR} (mm)	2.52	-0.33 (-13%)	0.49 (19%)	14308	3.09	-0.20 (-6%)	0.41 (13%)	18448

^a Number of values.

Table 4

Sources of climate variables used for reference evapotranspiration calculations in section 3.4.

Method	Acronym	Temperature	Solar radiation	Relative Humidity	Wind speed
Temperature Method	<i>HT</i>	Ground ^a			
Radiation Methods	<i>PT</i>	Ground	Sat ^b		
	<i>HR</i>	Ground	Sat		
	<i>TU</i>	Ground	Sat		
Penman-Monteith Method	<i>PM</i>	Ground	Ground	Ground	Ground

^a Ground : climate variable measured with the weather station devices.^b Sat : Helioclim-1 data (for solar radiation).

Table 5

Summary of statistical indexes of E_0 estimation methods, at daily time step. Values between brackets represent the bias and the RMSE divided by PM mean values (relative bias and relative RMSE). R^2 is the coefficient of determination; N_{SW} and N_{SE} are the number of observations for Southwest and Southeast area, respectively. Figures in bold correspond to the best performance in E_0 estimates, according to the index considered.

	Method	Southwest (Oceanic climate)			Southeast (Mediterranean climate)		
		R^2	Bias (mm)	RMSE (mm)	R^2	Bias (mm)	RMSE (mm)
January ($N_{SW}=1189$) ($N_{SE}=1577$)	<i>HT</i>	0.150	0.08 (11%)	0.34 (49%)	0.044	-0.12 (-12%)	0.56 (81%)
	<i>TU</i>	0.205	-0.15 (-22%)	0.37 (54%)	0.227	-0.23 (-23%)	0.53 (77%)
	<i>PT</i>	0.112	-0.29 (-42%)	0.43 (63%)	0.097	-0.57 (-59%)	0.76 (110%)
	<i>HR</i>	0.053	-0.16 (-23%)	0.42 (62%)	0.255	-0.17 (-18%)	0.49 (72%)
April ($N_{SW}=1153$) ($N_{SE}=1481$)	<i>HT</i>	0.668	0.17 (6%)	0.62 (22%)	0.348	-0.30 (-9%)	1.01 (36%)
	<i>TU</i>	0.830	-0.66 (-23%)	0.80 (28%)	0.672	-0.66 (-19%)	0.96 (34%)
	<i>PT</i>	0.816	-0.46 (-16%)	0.63 (22%)	0.672	-0.53 (-15%)	0.87 (31%)
	<i>HR</i>	0.825	-0.57 (-20%)	0.77 (27%)	0.678	-0.51 (-15%)	0.90 (32%)
July ($N_{SW}=1236$) ($N_{SE}=1497$)	<i>HT</i>	0.624	0.56 (13%)	0.96 (22%)	0.217	-0.53 (-9%)	1.32 (30%)
	<i>TU</i>	0.866	-0.42 (-10%)	0.65 (15%)	0.549	-0.77 (-13%)	1.19 (27%)
	<i>PT</i>	0.868	-0.05 (-1%)	0.50 (11%)	0.576	-0.30 (-5%)	0.93 (21%)
	<i>HR</i>	0.869	-0.13 (-3%)	0.67 (15%)	0.560	-0.18 (-3%)	0.97 (22%)
Year ($N_{SW}=14308$) ($N_{SE}=18448$)	<i>HT</i>	0.894	0.32 (-13%)	0.67 (28%)	0.804	-0.20 (-6%)	0.96 (31%)
	<i>TU</i>	0.914	-0.30 (-12%)	0.58 (24%)	0.880	-0.40 (-13%)	0.84 (27%)
	<i>PT</i>	0.938	-0.29 (-12%)	0.52 (22%)	0.890	-0.47 (-15%)	0.86 (28%)
	<i>HR</i>	0.906	-0.21 (-9%)	0.59 (24%)	0.882	-0.21 (-7%)	0.77 (25%)